J Mater Sci (2006) 41:6035–6045
DOI 10.1007/s10853-006-0511-z

A study on the carbon soot derived from the wood combustion and on the relative alkali-extractable fraction

A. Arrais · E. Diana · E. Boccaleri

Received: 3 May 2004 / Accepted: 18 August 2005 / Published online: 5 August 2006

Abstract In this experimental study, waste particulate of domestic flame combustion of wooden matters have been reacted according to a direct mild-condition reductive-oxidative chemical synthesis. Water-soluble graphenic and polycyclic aromatic frameworks have been extracted from graphitized carbon residues. Products have been recovered by elemental carbon contented in both fly and bottom combustion particulate. Their pH-sensitive behavior in aqueous solutions has been elucidated. Products and reactant substrates have been spectroscopically characterized by mean of solid state vibrational FT-IR and Raman, UV-VIS, XRD, solution ^{1}H and ^{13}C NMR, SEM-EDX and MALDI-TOF MS techniques. Discussion upon the reactivity of flame carbon residues of wooden matters is reported, in comparison to the reactivity displayed by other graphenic structures, according to the reported synthetic protocol.

Introduction

Flame combustion processes of wooden materials in fireplaces, ovens, boilers, stoves, etc., provide considerable extent (presently hundred thousands of tons/yr. per single advanced country only) of graphitized carbonaceous particles [1]. These matters, given by the incomplete combustion of the ligneous biomasses, are found in both residual bottom and fly ashes and result mixed together with all the other typical organic and inorganic flame by-products [2]. At present, the recycle of combustion wood waste media is focused essentially on the inorganic matter component. Reuse employment actually spans from the outdated traditional use of employing basic alkali salts contented in wood bottom ashes for the saponification of fat triglycerides [3] up to the recent usage of wood bio-fuel ashes in addressing acidification and sustaining regeneration of soils for agriculture and forestry [4]. Wood combustion carbon matter particulate, on the other hand, is usually regarded as a final useless waste material [5] and a further effort of systematic study about its peculiar structural features and its recycle potential is desirable. Such carbonaceous residues, actually, constitute an underestimated raw cheap source of graphenic and aromatic substrates, that could indeed provide functionalized polycondensed aromatic macromolecules and polycyclic aromatic hydrocarbon (PAH) frameworks, by mean of proper chemical treatments. Nowadays, functionalized polycondensed aromatic structures are indeed a coveted class of molecular materials, largely employed in chemical manufacturing [6]. Among much other, water-soluble carbon frameworks and PAHs find relevant assessed applications in the ambits of surfactant chemistry [7], wetting additives [8], phase-transfer catalysis [9], complexation molecular carriers [10], poly-electrolytic membranes [11] viable dyes and inks [12], drug-designed active agents and fluorescence markers in biochemistry [13]. At

---

A. Arrais (✉) · E. Diana
Dipartimento di Chimica Inorganica, Chimica Fisica e Chimica dei Materiali, Università degli Studi di Torino, Via Pietro Giuria 7, 10125 Torino, Italy
e-mail: aldo.arrais@unito.it

E. Boccaleri
Dipartimento di Scienze e Tecnologie Avanzate, Università del Piemonte Orientale "A. Avogadro", Spalto Marengo 33, 15100 Alessandria, Italy

present, from residual combustion carbon soot only a very minor fraction of the highly aromatic, lower-weighting humic acids [14] can be promptly extracted in alkali aqueous solutions.

Focusing on fullerenes, nanotubes and large poly-condensed molecules, we have been investigating the chemical reactivity of different unsaturated graphenic carbon networks towards the simple chemical processes of reduction and oxidation of the weakly delocalized C=C carbon double bonds, paving the way for a convenient achievement of a few water-soluble functionalized carbon frames [15–17]. The graphitization extents of elemental carbon that, as for the valuable carbon clusters case, occurs in flame combustion particulate of wood matters was therefore regarded by us with particular keen attention, as these carbon substrates can actually provide a cheap interesting raw material for a quantitative gross extraction of water-soluble aromatic structures. Moreover, the peculiar reactivity of this wooden-derived particulate is expected to be intrinsically dependent on the intimate structure of the defectively graphitized carbon matter contented, thus representing a further opportunity to explore the general reactivity of the carbon frames according to this method, on the basis of the actual graphitization extent.

In this paper, beside a comprehensive spectral characterization of carbon matter contented within flame combustion particulate of wooden matters, the successful convenient massive extraction and spectral characterization of water-soluble graphenic and poly-condensed aromatic derivatives obtained from such graphitized residues is reported. Based on spectral insights, a further discussion upon correlation between the chemical reactivity of these waste media and the defective structural graphitization of their carbon content is therein developed.

Experimental

Wood waste materials, reactants and solvents

Wood flame combustion ashes and the carbon particulate derive from residential fires of mixtures of several different hard wood matters (mainly oaks and ashes) of Eastern Piedmont (Alessandria, Italy). Several logs of approximately 40 cm length were burned in a common domestic fireplace, and the whole black deposited carbon particulate was straightforward collected throughout the initial 1.5 m chimney column. Other different flame carbonaceous residues of wood matters were provided by collecting black carbon soot contented within fire bottom ashes of conifer (pine and larch) of Cotiae Alps of Western Piedmont (Turin, Italy). Sodium lumps and potassium rods were purchased by Aldrich. The liquid alkali alloy Na/K was prepared in situ in a dry recipient and used immediately afterwards. Any contact with water and primary alcohols must be rigorously avoided. The volatile secondary isopropylic alcohol is suggested for safe slow decomposition of the alloy after use. All solvents was purchased by Riedel de Haën. Tetrahydrofuran (THF) was bubbled with an inert gas stream of Ar for 15 min before use. Deionized water was obtained by mean of a ion-exchange resin. TLC Silicagel60 was purchased by Merck.

Synthetic extraction of water-soluble derivatives from wood combustion carbon particulate

In a typical lab-scale experiment, using standard Schlenk techniques (0.150 L Schlenk tube, Ar), 2 g of wooden flame combustion residues were suspended in 10 mL of dry THF and ca. 0.1 g (i.e. 1–2 drops) of the liquid alkali alloy Na/K was added (CAUTION: please, keenly refer to details reported in the above materials section for a proper handling of the alloy Na/K). A silicon oil trap was connected to the tube, to maintain the anaerobic atmosphere and allow the eventual development of molecular hydrogen during the chemical reduction of the mixture. The mixture was stirred for 15 h under anaerobic conditions. It was then stirred for other 8 h under full aerobic atmosphere. 2–3 mL of isopropylic alcohol were added therein, to completely ensure the slow decomposition of the residual liquid Na/K alloy. Afterwards, 0.1 L of water was slowly poured into the Schlenk tube and the mixture was extracted by vigorous stirring for 4 h. It was successively filtered through a paper filter, to remove the water-insoluble residual particles; the resulting dark brown aqueous solution was slowly acidified at ca. pH 4 with a HCl aqueous solution. A suspended matter was now formed and the suspension was allowed to completely settle (16 h, 10 °C). The pale yellow surnatant solution, now containing Na/K chlorides and a few related hydrogen carbonates (the residual alkali alloy final decomposition products), was decanted and the remaining dark solid precipitate was washed with methanol and then dried for 2 h under vacuum (1 Pa). Being a hydrophilic, rather hygroscopic material, the evaluation of a precise yield of reaction is therefore somewhat awkward. By a gross estimate of the weights of carbonaceous reactant matter [1, 4] and vacuum-dried isolated products, a reliable average reaction yield is estimated to be up to about 70%.

Table 1 Summary of performed reactions and correlated experimental conditions tested for different wood-combustion carbonaceous substrates

Number of performed run reaction (substrate)	Type of tested reaction performed upon combustion carbon soot	Employed reactive metal agent	Total times (h) of reaction (R = Reduction; O = Oxidation)	Indicative yields (% wt) of water-soluble extracts[a]
Run1$_{\text{(fly soot)}}$	Reduction/oxidation	Na/K liquid alloy	23 (15 R + 8 O)	60
Run2$_{\text{(bottom soot)}}$	Reduction/oxidation	Na/K liquid alloy	23 (15 R + 8 O)	20
Run3$_{\text{(fly soot)}}$	Reduction/oxidation	K	30 (15 R + 15 O)	55
Run4$_{\text{((2) derivatives)}}$	Hydrogenation	$Zn + HCl \rightarrow H_2$	5	95

[a] Yields of reaction are here weighted with respect to the total amount of the starting reactant substrates, i.e. taking also into account for combustion products the weights of the residual combustion inorganic fractions

Additional extractions of the crude of reaction with water yielded supplementary extents of products.

Duplication of the procedure was achieved by applying the same synthetic protocol to the carbon residues embedded within wood matter combustion bottom ashes. Average yields of reaction with respect to the carbon content are expected to be similar to the precedent reported case, although the higher content of the mixed inorganic residues within bottom ashes obviously lowers the actual yield of water-soluble products obtained, with respect to the total amount of the starting reacted matter.

Chemical reductions of substrates employing metallic potassium uniquely were also successfully tested within the protocol, although best results from a kinetic perspective are achieved by taking profit of the surface-renewable, liquid chemical alloy Na/K. Increasing amounts of the reducing agent were indeed consistently found to shorten reaction times.

Chemical further hydrogenation of water-soluble derivatives was performed by bubbling a stream of H_2 (generated by a drop-wise slow percolation of a dilute HCl solution upon metal Zn) for 5 h in a flask containing 5 mL of water solution of the stirred pristine hydrophilic derivatives (NaOH pH 8, 35 °C). A dark red water-soluble matter is achieved. A summary of all performed reactions with correlated experimental conditions is reported in Table 1.

Instrumental

Solid state FT-IR spectra were performed on a Bruker Equinox 55 spectrophotometer (KBr discs, 2 cm^{-1} spectral resolution). KBr has been stored in a drying oven at 110 °C for 4 h before use. Blank spectra of KBr discs are reported in Figs. 3(a) and 7(a), to confirm the substantial absence of adsorbed humidity upon detected KBr matrixes. Raman spectra were collected on a Bruker RFS 100, equipped with a 1.064 μm Nd:YAG laser as the exciting source (15,000–20,000 scans, laser powers set in the range 30–180 mW, with spectral resolution set at 4 cm^{-1}). Solution UV-VIS electronic spectra (H_2O) were obtained on a Perkin Elmer λ 900 double-ray spectrophotometer. XRD spectra were obtained on a Thermo ARL X-ray diffractometer, operating with a $1.540562 \cdot 10^{-1}$ nm $CuK_{\alpha 1}$ X-ray radiation (X-ray generator current and voltage set at 40 mA and 45 kV). ^{1}H-NMR and ^{13}C-NMR solution spectra were acquired on a JEOL EX 400 MHz spectrometer; the resonance values are given in ppm versus the external tetramethylsilane (TMS) reference. Energy Dispersive X-ray (EDX) elemental analysis was evicted on a SEM/EDX Leo1450 VP scanning electron microscope (electron probe gun set at 15 mm from the target, electron probe current within the range 3,100–3,440 A, with accelerating voltage set at 15 and 20 kV); the analysis were performed upon several 6×10^{-2} mm^2 portions of 1 mm-thick, 1 mm-diameter pellets of the powdered-pressed materials. MALDI-TOF MS measurements were acquired on a Bruker Reflex III spectrometer, equipped with a 337 nm N_2 laser as the excitation source (ion acceleration voltage set at 25.00 kV, reflector voltage 28.70 kV, first extraction plate 20.90 kV).

Results and discussion

Spectral characterization of wood combustion carbon particulate

All spectral analysis performed upon carbonaceous residues of wood matters combustion are peculiarly representative of the incomplete oxidative processes that generate heterogeneous complex matters, intimately constituted by graphenic carbon particulate (**1**), mixed with traces of non-volatile organic hydrocarbons and a variable extent of inorganic salt by-products. Carbon particulate exhibit a structural extent of defective graphitization, showing the typical spectral patterns which fairly resemble those of industrial glassy carbons and carbon blacks [18]. A typical average elemental composition, obtained by SEM-EDX analysis of the carbonaceous flame particulate residues, indicated for the examined carbon matter a main expected contamination provided by calcium and a few potassium inorganic salts [4], and the evicted total oxygen content suggested as well that a notable extent of oxygen units are also covalently retained upon the carbon network (**1**). The XRD diffraction profile of (**1**) is reported in Fig. 1(a). It shows features that are substantially representative of the glassy graphitization of residual carbon. It is fairly dominant the broadened hump with the maximum set at 21.6 2θ, that is indicative of the disordered graphitic frameworks [19]. The remaining lesser sharp peaks are assignable to the collected inorganic by-product calcium carbonate. Raman spectrum of (**1**) supports such indications about disordered carbon graphenes, displaying two broad bands of approximately equal intensities set at 1,580 and 1,310 cm^{-1}, that are reported in Fig. 2(a). The former peak is referred to the skeletal breathing modes of graphenic moieties, whilst the latter is a band that becomes furthermore active in disordered graphite and glassy carbons, due to the presence of several structural defects in graphene layers. [20, 21] A representative FT-IR spectrum of wood combustion carbon particulate is illustrated in Fig. 3(b). Contamination of inorganic alkali residues of (**1**) are immediately evident when observing the strong broad band set ca. 3,430 cm^{-1}, that is indicative of νO–H stretching modes. The organic carbonaceous residues of (**1**) display a few peculiar absorptions, whose peaks were measured at 1,725 cm^{-1}, that is suggestive of a few ketonic νC=O stretching modes, at 1,610 cm^{-1}, that is consistent with νC=O carbonylic stretching modes of anionic carboxylates and at 1,110 cm^{-1}, that is representative of νC–O stretching modes of ether groups [22]. Albeit an absorption in this spectral region might be consistently indicative of conjugated νC=C moieties, the broad band set at 1440 cm^{-1} results however well referable to the presence of inorganic carbonates in the examined matter, whilst, from the point of view of the carbon content, a partial extent of retained carbon hydrogenation is observed, as it is evicted by inspecting the small bands in the range 3000–2850 cm^{-1} (typical of aliphatic νC–H stretching modes) and the broad indented absorption appearing at 750 cm^{-1} (consistent with γC–H bending modes) [23]. Finally, the peculiar sharp bands that are visible in the range 1000–600 cm^{-1} appear to be again due to contamination of inorganic by-products, the 875 and 712 cm^{-1} bands being reasonably indicative of calcium and a few alkali carbonates [22] and the 818 cm^{-1} band being presumably due to an impurity extent of silicates in the collected examined matrix [4]. For extensive information, in Fig. 3(d), a FT-IR spectrum of wood

Fig. 2 Raman spectra of (**1**) (**a**) and (**2**) (**b**)

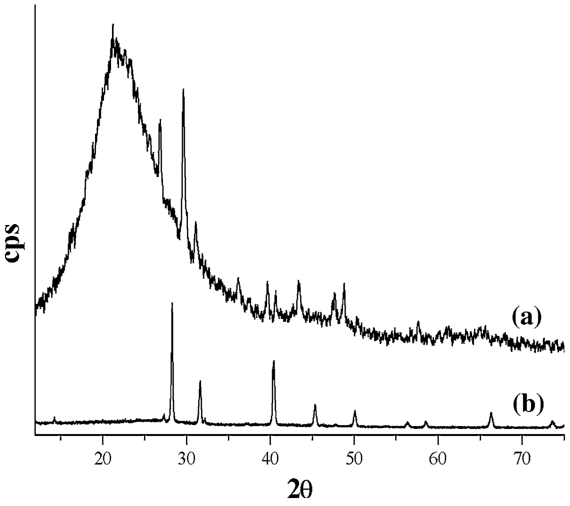

Fig. 1 XRD patterns of (**1**) (**a**) and (**2**) (**b**)

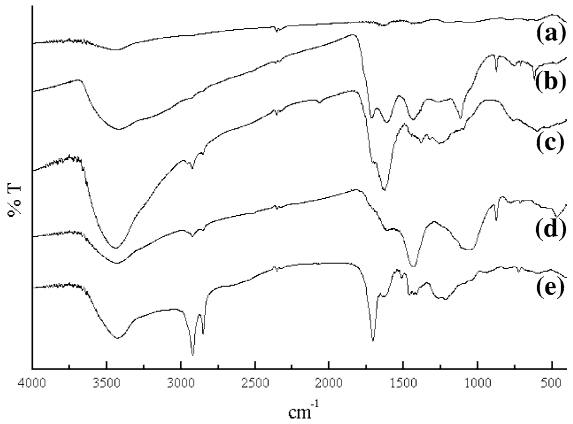

Fig. 3 FT-IR spectra (KBr discs) of KBr (**a**), (**1**) (**b**), (**2**) (**c**), (**1′**) (**d**) and (**2′**) (**e**)

combustion bottom ashes is reported. Within this incinerated substrate, more evidently than the former case, the patterns of consistent inorganic matters are predominant, with the expected massive presence of calcium carbonate. However, the ash-embedded organic frames and carbonaceous particulate content, that are similarly indicated as **(1′)**, are reliably suggested by the broad absorption hump at ca. 1,050 cm^{-1}, that is indicative of stretching modes of νC–O units, and by the wide indented pattern in the 1,770–1,520 cm^{-1} interval, that is referable to both νC=O stretching modes of ketonic and carboxylic moieties and to νC=C stretching modes of the carbon frames.

The comprehensive collected spectral results indicate that carbon matters in waste particulate provided by flame combustion of wooden materials display a glassy carbon-like structure, still retaining a few extents of partially oxidized and hydrogenated organic carbon frameworks [24]. All these units may well derive from the incomplete combustion processes of wooden substrates. On the purpose, in Fig. 4, a reliable general schematic representation of (**1**) is suggested.

By suspending collected particulate in water, the residual inorganic fraction is efficiently extracted, giving a basic solution, while only an exiguous extent of the carbon fraction (**1**) contented in the incinerated waste material mixture can be solved, i.e. the polyaromatic humic acidic fraction [14], possibly conferring to the water solution a pale yellow color. Carbonaceous residues, even so, results to be on the whole poorly water-soluble and substantially unaffected by pH-variations.

Spectral characterization of water-soluble derivatives from wood combustion carbon particulate

The reported chemical treatment of carbon particulate contented in wood flame combustion particulate provides high yields of hydrophilic, moisture sensitive water-soluble derivatives (**2**), displaying an average H_2O solubility of about 1–1.5 mg/mL in ca. neutral solutions. The main striking feature of (**2**) in aqueous media is their sensitive pH-dependent behavior. Actually, mild and strong basic conditions afford a higher solubility, up to more than one order of magnitude (i.e., at pH ca.10 the solubility of (**2**) in water is raised at about 20–25 mg/mL), whereas shifting towards progressively acidic conditions the solubility results furthermore hampered, the massive precipitation of (**2**) beginning at about pH ≤ 5. The observed experimental trends are in full accordance with the presence in (**2**) of carboxylic units, which can be deprotonated or protonated, accordingly to the respectively basic and acid conditions, thus therefore influencing the resulting hydrophilicity of the products, by displaying a hydrophilic anionic, or a less polar neutral moiety.

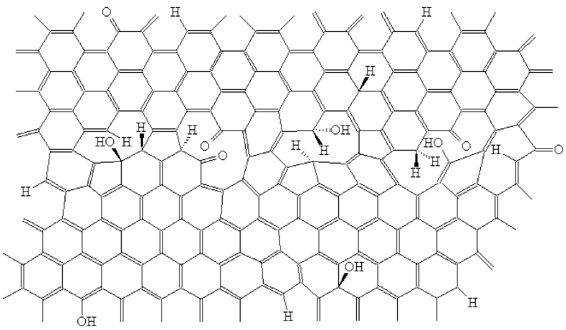

Fig. 4 General schematic representation of wood flame combustion carbon particulate (**1**). Structural and terminal saturation defects are illustrated

The evicted average elemental composition (SEM-EDX) of the obtained water-soluble derivatives (**2**) is informative of the achieved oxygen content in hydrophilic frames, roughly estimable at about 4:1 C:O ratio. The only significant evaluated by-products (observed up to 3% of the total atom abundance) are sodium and potassium chlorides, that are residual contaminants provided by the isolation procedure of (**2**), together with small traces of calcium chlorides, that may derive from the initial contamination of (**1**).

The XRD diffraction pattern of (**2**) is showed in Fig. 1 (b). If compared to that exhibited by (**1**), this latter does not display any significant signal due to carbonaceous frames, but a few sharp peaks related to the inorganic salts residual impurity (i.e., basically NaCl and KCl) that remain after the isolation of the investigated derivatives. The result suggests for (**2**) a marked enhancement of the amorphous nature of the products due to the chemical dispersion of attached structural functionalities.

Given the high solubility of (**2**) in basic water solutions, a ^{13}C NMR spectrum of (**2**) has been recorded in D_2O solution basified at ca. pH 10 with NaOD. The resulting spectrum is reported in Fig. 5. The absorption set at about 175 ppm suggests the presence upon (**2**) of C=O carbonylic moieties; the weak peak at ca. 148 ppm can be referred to the carbon atoms belonging to the anionic carboxylate units. The large indented absorption comprised in the range 135–105 ppm is related to different unsaturated sp^2 carbon atoms; the adjacent absorptions in the range 105–85 ppm, displaying a maximum at about 95 ppm may be due to a dispersion of several alcoholic functions. Finally, the strong peaks at low fields, set in the range 40–20 ppm, refer to an extent of hydrogen-saturated aliphatic

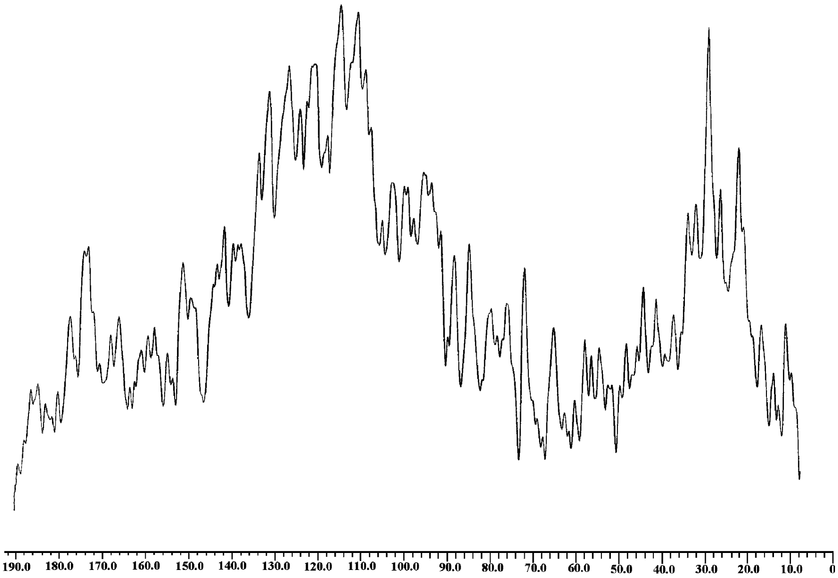

Fig. 5 ^{13}C-NMR solution spectrum of (**2**) (D_2O solution, NaOD pH 10)

carbon units [25]. It is interesting to notice that the spectral pattern obtained in D_2O basic solution roughly resembles the one obtained in solid state for water-soluble derivatives of other carbon substrates, obtained through the same reactive chemical protocol [16].

D_2O solution ^{1}H-NMR signals are gravely hampered by the isomeric dispersion of bonded functionalities upon (**2**) and by the potential presence of mobile protons. Proton-exchange with the deuterated water, however, has been assessed. A ^{1}H standard reference of $CHCl_3$, sealed inside a glass capillary, was used to measure, by mean of signal integration, the intensity of the contaminating DHO peak in the deuterated D_2O solvent. The spectrum of neutral (**2**) was consequently recorded in the same D_2O solution. The increase of such peak, passing from a DHO/$CHCl_3$ ratio of 0.39175 observed in the blank to a DHO/$CHCl_3$ ratio of 0.54225 observed in the (**2**) D_2O solution, represents a clear evidence of the proton-exchange between the deuterated solvent and a few mobile protonic functionalities implanted upon (**2**), reasonably belonging to alcoholic and carboxylic oxygenated moieties. [17, 26]

Solid-state Raman spectrum of (**2**), illustrated in Fig. 2(b), detects the persistence of C=C moieties belonging to disordered delocalized graphenic structures that were yet evaluated in the reactant carbon matter (**1**): the two diagnostic broad bands at 1,580 and 1,310 cm^{-1} are again visible, being the two Raman patterns of (**1**) and (**2**) nearly super-imposable [17, 20].

A representative FT-IR spectrum of (**2**) is showed in Fig. 3(c). The very strong absorption of (**2**) showing its maximum at about 3,480 cm^{-1} displays a narrower and stronger pattern, if compared to that exhibited by wood ash residues (Fig. 3(b)), being representative of the organic νO–H stretching modes of alcoholic and carboxylic units that are now attached to (**2**). The second strong shouldered band set at ca. 1,600 cm^{-1} is consistent with the massive attachment of carboxylic units, as the typical strong νC=O stretching modes of such groups fall in the 1,650–1,580 cm^{-1} range. The upper shoulder at about 1,720 cm^{-1} is referable to the presence of νC=O stretching modes of ketonic units. The wide broadened absorption pattern in the range 1,400–1,000 cm^{-1} can be referred to νC=C stretching modes of residual skeletal conjugated carbon frameworks and δC–OH bending modes (in the 1,400–1,200 cm^{-1} zone) and to νC–O stretching modes (in the 1,200–1,000 cm^{-1} zone) [21]. In the spectral pattern of (**2**), none of the sharp peaks that were visible in the FT-IR spectrum of (**1**) (and attributed to inorganic by-products contamination) are observable and the reacted hydrophilic material appears now to be constituted by a dispersion of several isomeric different organic functionalities. Fig. 3(e) shows the vibrational profile of the related water-soluble derivatives (**2′**), obtained by wood flame combustion carbon matter (**1′**) embedded in bottom ashes. The hydrophilic products display the same oxygen moieties yet evicted in (**2**). It is perhaps interesting to notice that in (**2′**) a marked aliphatic absorption pattern is present, alongside to a relatively hampered νO–H band and with an inverted ratio between the intensity of the ketonic and carboxylic bands, if compared to that displayed by (**2**). These comprehensive spectral results possibly seem to suggest for (**2′**) the occurrence of tautomeric keto-enolic equilibria of vinyl-alcoholic moieties.

In Fig. 6(a) the UV-VIS spectrum of (**2**) measured in H_2O solution in the range 180–750 nm is illustrated.

The observed continuum of absorption displaying its maximum at about 180 nm [16, 17] is concordant with other previous reports about similar carbon matters, reacted according to this protocol. It seems interesting a comparison between the electron spectrum of (**2**) and the previously unreported one that is referred to water-soluble derivatives of fullerene C_{60} (reported in Fig. 6(b)), achieved by the same synthetic route [14]. It appears therein immediately evident for (**2**) the presence of a very broad shoulder in the range 200–450 nm, that is on the contrary absent in the case of the carbonaceous products that derive from one single molecular carbon framework of buckminsterfullerene C_{60}. This broadening of the electron absorption pattern seems to be basically indicative of the wide chemical dispersion of unsaturated residual frameworks C=C that are yet present in the reactant matters (**1**). Conversely, the observed similar UV strong peaks at ca. 180 nm, that are evaluated both for (**2**) and C_{60} water-soluble derivatives, appear to be representative of the different attached organic oxygenated moieties, both alcoholic and carboxylic or ketonic [27]. However, partial hydrogenation of (**2**) has been chemically attempted. The related solid-state FT-IR spectrum of the resulting neutralized water-soluble products (**3**) is reported in Fig. 7(b). Enhancements of the peculiar vibrational bands set in the 2,950–2,800 and 1,400–1,250 cm^{-1} ranges, that are assigned to the stretching *v*CH and bending *δ*CH modes of aliphatic C–H units appear visible. Furthermore, the relative intensity of the 1600 cm^{-1} band results now consistently hampered in (**3**) when compared to the intensities of the absorption in the 1,400–1,000 cm^{-1} range, and the disappearance of the upper shoulder at ca. 1,720 cm^{-1} is observed. These data suggest that a main hydrogenation of the ketonic groups should reasonably take place in (**3**), thus enhancing the average number of alcoholic functionalities, with the absorption in the 1,200–1,000 cm^{-1} range, due to *v*C–O stretching modes that appears consistently enforced [22].

The whole of collected spectral data suggests that several polar oxygen moieties are implanted upon hydrophilic aromatic carbon frameworks. The observed isomeric structural moieties of fire carbon particulate (**1**) results even more dispersed by the further isomeric insertions of oxygenated units upon graphenic frames, as it can be clearly resumed by vibrational and XRD analysis.

The oxidation of reduced graphene structures

The investigated water-soluble materials appear to derive from the graphitized carbon frameworks formed alongside during the flame oxidative processes of wooden matters (refer to Fig. 4). The graphenic sp^2 C atoms actually result to be a proper target to bear an electron reduction, provided by the liquid alkali alloy, allowing its delocalization throughout the whole C=C unsaturation network. Such electron incorporation can herein favor the further electrophilic oxidation of substrates provided by atmospheric O_2. Therefore, it seems reliable to assume a plausible two-step chemical mechanism, that begins with electron reduction of the delocalized graphenic framework and results in subsequent aerobic oxidation of these latter provided by atmospheric molecular dioxygen insertions. Despite atmospheric moisture traces are reasonably responsible of the ending protonation for the attaching oxygen units, however the major amount of atmospheric dioxygen favors the stepwise addition of different hydroxylic and carbonylic moieties upon reduced graphenic matters. In Fig. 8, a general reactive path for the achievement of water-soluble oxygenated aromatic frameworks is tentatively proposed.

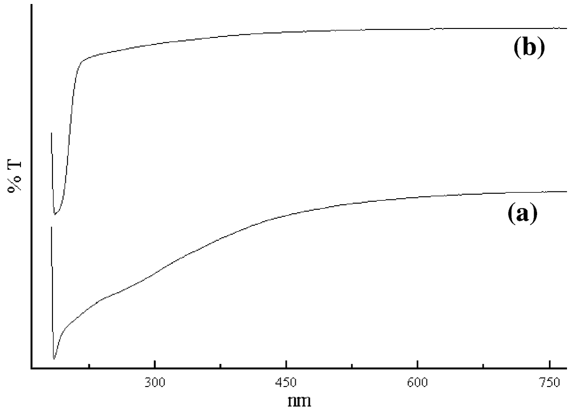

Fig. 6 UV-VIS spectra (H_2O solution) of (**2**) (**a**) and C_{60} water-soluble derivatives (**b**)

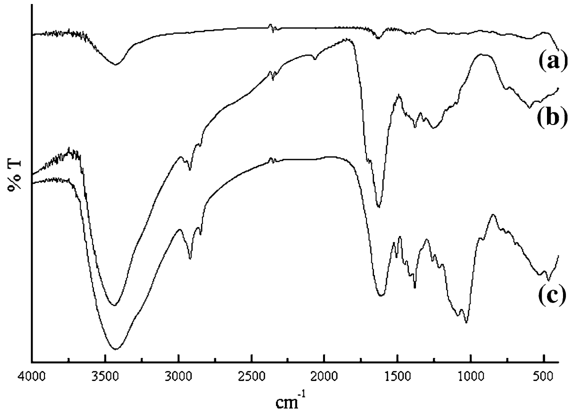

Fig. 7 FT-IR spectra (KBr discs) of blank KBr (**a**), (**2**) (**b**) and hydrogenated water-soluble derivatives (**3**) (**c**)

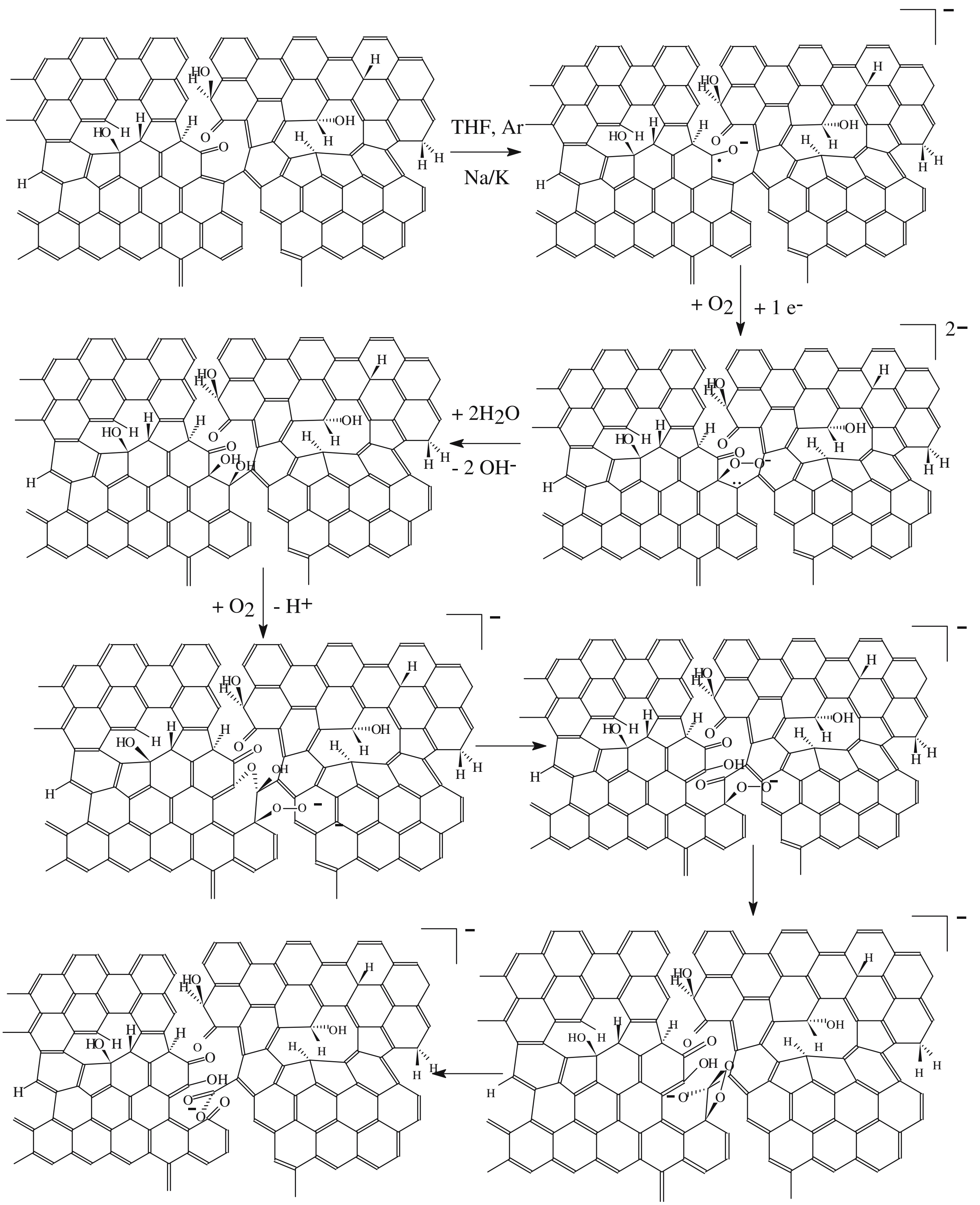

Fig. 8 Proposed schematic reaction mechanisms of oxygen moieties insertion and oxidative cleavage of graphenic network of (**1**) to generate fragmented water-soluble aromatic frames (**2**)

Within this matter context, it is on form reliable that partial degrees of disorder in graphitized flame particulate can favor extensive oxidation of the carbon substrates. In fact, contrary to the ordered graphite model, the skeletal framework of (**1**) results provided with several structural defects; i.e., pentagonal rings, heptagonal rings, hydrogen and oxygen saturations, surface plain terminations, etc. (refer to Fig. 4). They are all factors that confer to the carbon substrate a marked extent of tensional and torsion strains and structural deformations [24], with a consequent comprehensive low resonance energy of the C=C double bonds of the glassy graphitized carbon matters (**1**). Considering such frames, both electron delocalization, from one side, and the low resonance energy, on the other one, may act in concert for an easy oxidation of the starting substrates. Credibly, whereas the unsaturated graphenic frameworks allow by mean of electron delocalization the feasible electron incorporation provided by the metallic reducing agent, on the other hand the low resonance energy due to the disordered and defective carbon graphitization promote a prompt O_2 oxidation of the same reduced C=C frames by electrophilic insertion, during aerobic exposure [28]. Accordingly, it results mostly probable that oxygen electrophilic attachments should primarily take place upon the most isolated and least delocalized C=C bonds, displaying the highest energy strains and the lowest degree of resonance energy. On the purpose, all such considerations are actually well supported by the experimental observations concerning the average higher yields of reaction products (**2**) and (**2′**) that are achieved by applying the reductive/oxidative protocol to a disordered graphenic carbon substrate, rather than to a regularly ordered carbon network. It is as well furthermore plausible that both the coalescence shielding among carbonaceous reactant particles and the steric hindrances of the starting graphenic substrates may in addition also play an active role in generating and preserving all the experimentally observed oxygenated hydroxylic, ketonic and carboxylic moieties.

As a line of principle, an additional contribution to the yields of reaction given by humic acids [14, 29] and by the upper PAH frames and a few Volatile Organic Compounds (VOC, that is, mainly substituted guaiacols and syringols) [1] that are formed in flame oxidative mechanisms of wooden materials cannot be excluded here. However, the low levels at which the smallest volatile structures are retained in the larger collected particulate after combustion processes, together with the enhanced reactivity displayed by the residual graphitized carbon particulate, tend to indicate this latter substrate as the actual privileged target matter of reaction. Besides, the investigated protocol may result as well effective in enhancing the oxygen content of the yet partially oxidized and fragmented carbonaceous structures, as the humic acid fractions [14], thus favoring their massive water-solubility [29], because of further attachment of polar oxygenated functions to the carbon frames.

As it has been previously discussed for carbon nanotubes substrates, within the reactive pathway context, fragmentation process [26, 30] of graphenes acts again a crucial role in extracting massive yields of functionalized hydrophilic lower-weighting frameworks. Contrary to the molecular carbon structure case, this collateral reaction phenomenon can be here experimentally profited and managed, by prolonging for the reactants the aerobic time of stirring in presence of the reducing agent Na/K, during which the oxidative cleavages of graphenic moieties should reasonably take place. Indeed, given a consistent oxygen extent yet present upon reactant matters (**1**), as it was evaluated by the SEM-EDX analysis, the efficiency of the solubilizing method in this peculiar case seems to stand properly in the ability of structural fragmentation of graphene moieties and concomitant extensive carboxylation of frameworks that are possibly achieved during the aerobic oxidative step (refer to Fig. 8). Within this perspective, it appears possible that increasing amounts of the reducing agent, as well as prolonged reduction times, might favorably affect the extent of fragmentation of the isolated water-soluble products. A straightforward TLC elution of (**2**) with a 1:1 H_2O/CH_3OH mixture upon a TLC Silicagel plate shows that the several isomeric products continuously broaden within a single wide brown band, eluting right after the solvent front. As it was yet performed for the previously reported cases [15–17], MS analysis to somewhat recognize a range of weight distributions due to fragmentation was therein acquired, employing the MALDI-TOF MS technique. A methanol solution of (**2**) was employed to prepare the sample. In the positive reflection ion mode acquisition, an extent of extracted molecular frameworks was displayed within the range 200–500 m/z. The highest ion peaks in the fragmentation groups were set at 227.84 (most intense), 249.83, 265.81, 288.15, 304.16, 316.20, 416.92, 476.80, 492.77 m/z. Since the low solubility of (**2**) in CH_3OH, it may be probable that within the products dispersion the smaller frames were preferentially detected.

Conclusions

In previous works, we have pointed out the efficiency of this protocol of chemical reduction and further air-oxidation for pure elemental allotropes of carbon, such as fullerenes and carbon nanotubes, as well as for related aromatic hydrocarbon frames. In the examined case, the reacting carbon matter within the engaged substrates is here provided by graphenic substrates given by defective flame combustion oxidative mechanisms of wooden materials. The residual elemental carbon left in wood combustion waste particulate resembles the disordered structural carbonaceous frameworks of glassy carbon and carbon blacks, that are conversely obtained through parallel pyrolitic mechanisms [31] from most different carbon fuels. It constitutes, with a possible co-participation represented by humic acids, upper PAH frames and VOCs, a proper reaction target for the application of the reductive/air-oxidative method. The few following conclusions can be herein drawn:

- massive high yields of water-soluble aromatic frameworks are conveniently extracted from the carbon content of wood combustion wastes, by simple mean of a direct one-pot reductive/oxidative method, in which oxidation of the reduced substrates is achieved by mere air-exposure;
- the method appears to be essentially independent from the type of raw wooden matter employed in flame combustion, since the afterwards generated graphitized carbon particles are properly the actual substrate of the explored functionalizing and fragmenting reaction;
- water solubility is provided by inserted oxygen functionalizations and, mostly, by the fragmentation of carbon substrates, through several linkages of hydroxylic, ketonic and carboxylic moieties, that confer to the products a pH-sensitive behavior in aqueous media and render them interesting materials and precursors for further chemical functionalization;
- more investigation will allow to better discriminate within wood combustion waste materials the single reactive contributions given by the residual elemental carbon fraction and by humic acid structures, upper PAH and VOC frameworks formed during flame processes, in order to further illustrate the general reactivity of different unsaturated carbon substrates towards the examined synthetic protocol.

Acknowledgements Fund grant (FIRB) from the Ministero dell'Istruzione, Università e Ricerca is courteously acknowledged. Authors are grateful to Dr. Simonetta Geninatti Crich and to Dr. Davide Corpillo (Dept. Chimica I.F.M., University of Turin), for the performing of ^{13}C-NMR and MALDI-TOF MS spectra. Ing. Dario Pezzini (Poli@l CS^{2}M^2, Politecnico of Turin, Alessandria campus) is acknowledged for helpful assistance in SEM-EDX measurements.

References

1. (a) Hedberg E, Kristensson A, Ohlsson M, Johansson C, Johansson PÅ, Swietlicki E, Vesely V, Wideqvist U (2002) Atm Environ 36:4823; (b) Schauer JJ, Kleeman MJ, Cass GR, Simoneit BRT (2001) Environ Sci Technol 35:1716; (c) Mcdonald JD, Zielinska B, Fujita EM, Sagebiel JC, Chow JC, Watson JG (2000) Environ Sci Technol 34:2080; (d) Rogge WF, Hildemann LM, Mazurek MA, Cass GR (1998) Environ Sci Technol 32:13
2. (a) Skodras G, Grammelis P, Samaras P, Vourliotis P, Kakaras E, Sakellaropoulos GP (2002) Fuel 81:547; (b) Ross AB, Jones JM, Chaiklangmuang S, Pourkashanian M, Williams A, Kubica K, Andersson JT, Kerst M, Danihelka P, Bartle KD (2002) Fuel 81:571
3. Routh HB, Bhowmik KR, Parish LC, Witkowski JA (1996) Clin Dermatol 14:3
4. (a) Bohlin F, Roos A (2002) Biomass Bioenerg 22:237; (b) Demeyer A, Voundi Nkana JC, Verloo MG (2001) Bioresource Technol 77:287
5. (a) Hays MD, Smith ND, Kinsey J, Dong Y, Kariher P (2003) J Aerosol Sci 34:1061; (b) Saito M, Amagai K, Ogiwara G, Arai M (2001) Fuel 80:1201; (c) Barrefors G, Petersson G (1995) Chemosphere 30:1551
6. (a) Harvey RG (1997) Polycyclic Aromatic Hydrocarbons Wiley-VCH, New York pp 667; (b) Bjørseth A (ed) (1993) Handbook of polycyclic aromatic hydrocarbons. Marcel Dekker, Inc., New York pp 727
7. Rosen MJ, Dahanayake M (2000) Industrial utilization of surfactants: principles and practice. AOCS Press, Champaign pp 176
8. Reemtsma T (1996) J Chromatogr A 733:473
9. Park H, Jeong BS, Yoo MS, Lee JH, Park B, Kim MG, Jew S (2003) Tetrahedron Lett 44:3497
10. (a) Kamegawa K, Nishikubo K, Kodama M, Adachi Y, Yoshida H (2005) Colloid. Surface A 254:31; (b) Aulenta F, Hayes W, Rannard S (2003) Eur Polym J 39:1741; (c) Kikuchi J, Ariga K, Murakami Y (2001) J Supramol Chem 1:275
11. (a) Bayramoğlu G, Kaya B, Arica MY (2002) Chem Eng Sci 57:2323; (b) Ye X, Levan D (2003) J Membrane Sci 221:147; (c) Ye X, Levan D (2003) J Membrane Sci 221:163
12. (a) Ertekin K, Karapire C, Alp S, Yenigül B, Içli S (2003) Dyes Pigments 56:125; (b) Venkata MS, Chandrsekthar RN, Krishna PK, Karthikeyan J (2002) Waste Manage 22:575
13. (a) Da Ros T, Prato M (1999) Chem Commun 663; (b) Banik BK, Becker FF (2001) Bioorgan Med Chem 9:593; (c) Tatsu Y, Yamamura S (2002) J Mol Catal B-Enzym 17:203
14. Haumaier L, Zech W (1995) Org Geochem 23:191
15. Arrais A, Diana E (2003) Fuller Nanotub Car N 11:35
16. Arrais A, Diana E (2003) Synthetic Commun 33:3331
17. Arrais A, Boccaleri E, Diana E (2004) Fuller Nanotub Car N 12:789
18. Wang X, Zhang GM, Zhang YL, Li FY, Yu RC, Jin CQ, Zou GT (2003) Carbon 41:188
19. Yamada K (2003) Carbon 41:1309
20. Goto A, Kyotani M, Tsugawa K, Piao G, Akagi K, Yamaguchi C, Matsui H, Koga Y (2003) Carbon 41:131
21. Nakamizo M (1991) Carbon 29:757
22. Socrates G (2001) Infrared and Raman characteristic group frequencies, 3rd edn. John Wiley and Sons, Chichester pp 347
23. Langhoff SR (1996) J Phys Chem 100:2819
24. Cataldo F, Pontier Johnson MA, (2000) Fuller Nanotub Car N 10:1

25. Pouchert CJ, Behnke J (eds) (1993) The Aldrich Library of 13C and 1H FT NMR spectra, 3 Vols, 1st edn. The Aldrich Chemical Co., Milwaukee, p 4300
26. Cataldo F, Heymann D (2000) Polym Degrad Stab 70:237
27. Organic electronic spectral data, vol 1–31 (1960–1989) Wiley-Interscience Publishers, New York
28. Ghigo G, Maranzana A, Tonachini G, Zicovich Wilson C, Causà M (2004) J Phys Chem B 108:3215
29. (a) Klucacova M, Pekar M (2005) Colloid Surface A 252:157; (b) Kandrac J, Hutta M, Foltin M (1996) J Radioan Nucl Ch Ar 208:577; (c) Watanabe A, Itoh K, Arai S, Kuwatsuka S (1994) Soil Sci Plant Nutr 40:601
30. (a) Vander Wal R, Tomasek AJ (2003) Combust Flame 134:1; (b) Backreedy R, Jones JM, Pourkashanian M, Williams A (2001) Faraday Discuss 119:385
31. Asakura R, Morita M, Maruyama K, Hatori H, Yamada Y (2004) J Mater Sci 39:201